Spherical triboelectric nanogenerator based on spring-assisted swing structure for effective water wave energy harvesting

Xi Liang [a,b,1], Zhirong Liu [a,b,1], Yawei Feng [a,b], Jiajia Han [a,b], Linlin Li [a,b], Jie An [a,b], Pengfei Chen [a,b], Tao Jiang [a,b,c,*], Zhong Lin Wang [a,b,c,d,*]

[a] CAS Center for Excellence in Nanoscience, Beijing Key Laboratory of Micro-nano Energy and Sensor, Beijing Institute of Nanoenergy and Nanosystems, Chinese Academy of Sciences, Beijing 101400, PR China
[b] School of Nanoscience and Technology, University of Chinese Academy of Sciences, Beijing 100049, PR China
[c] CUSPEA Institute of Technology, Wenzhou, Zhejiang 325024, PR China
[d] School of Materials Science and Engineering, Georgia Institute of Technology, Atlanta, GA 30332-0245, USA

ARTICLE INFO

ABSTRACT

Ocean wave energy is one of the most promising clean and renewable energy sources, so developing effective methods to collect such 'random' and ultra-low frequency energy is indispensable. The invention of triboelectric nanogenerators (TENGs) provides new prospects for large-scale blue energy harvesting. In this work, a new spherical TENG based on the coupling of spring-assisted structure and swing structure, integrated with a charge excitation circuit (CEC), was constructed to scavenge water wave energy. The particular structure can transform low-frequency water wave vibrations to high-frequency motions, elevating the frequencies of electrical outputs. Moreover, a TENG array consisting of four TENGs with CECs was fabricated, exhibiting a maximum output power of 16.6 mW and a 205 times enhanced output current of 23.3 mA. The charge excitation TENG array was demonstrated to successfully power a digital thermometer and a wireless signal transmission and reception system without any external power supply. Our study not only provides a new type of TENG with improved performance, but also offers a strategy for constructing maritime internet of things (IoTs) system.

1. Introduction

Energy source crisis is a common issue today faced by all countries around the world. For the sustainable development of human society, the exploitation of advanced energy technologies becomes the focus of energy research [1]. The turbulent ocean waves contain tremendous clean and renewable energies, which deserve to be exploited [2]. For decades, various schemes have been proposed based on traditional electromagnetic generators (EMGs) to collect ocean wave energy [3,4]. However, those experimental apparatuses are almost inefficient under low-frequency ocean waves (< 2 Hz). The EMGs are also confronted with the disadvantages of heavy mass, high cost, and easy to corrode [4, 5]. Therefore, developing other more efficient technologies for water wave energy harvesting is the key to breaking down barriers.

Triboelectric nanogenerator (TENG, also called as Wang generator) was invented in 2012 as a promising technology for converting

mechanical energy into electrical power [6,7]. Compared with the EMGs, the TENGs do not rely on bulky magnetic components. They adopt a working mechanism of Maxwell's displacement current [8], so they are more flexible, lightweight and cost-effective [9–12]. So far, the TENGs have exhibited huge potential in harvesting energy from a variety of sources, especially the low-frequency ocean waves [13–23]. However, for most demonstrated TENG devices, the water waves with ultra-low triggering frequency can only induce TENGs to generate electrical outputs at the similar frequency, resulting in insufficient energy conversion [24,25]. In our previous works, two effective solutions have been proposed to multiply the output frequency, respectively by introducing springs to store elastic potential and constructing pendulum-like structures capable of continuous swing [24,26–28]. Based on these studies, the more optimized structure needs to be further designed. Besides amplifying the output frequency, investing efforts to enhance the output current is also important for large-scale practical
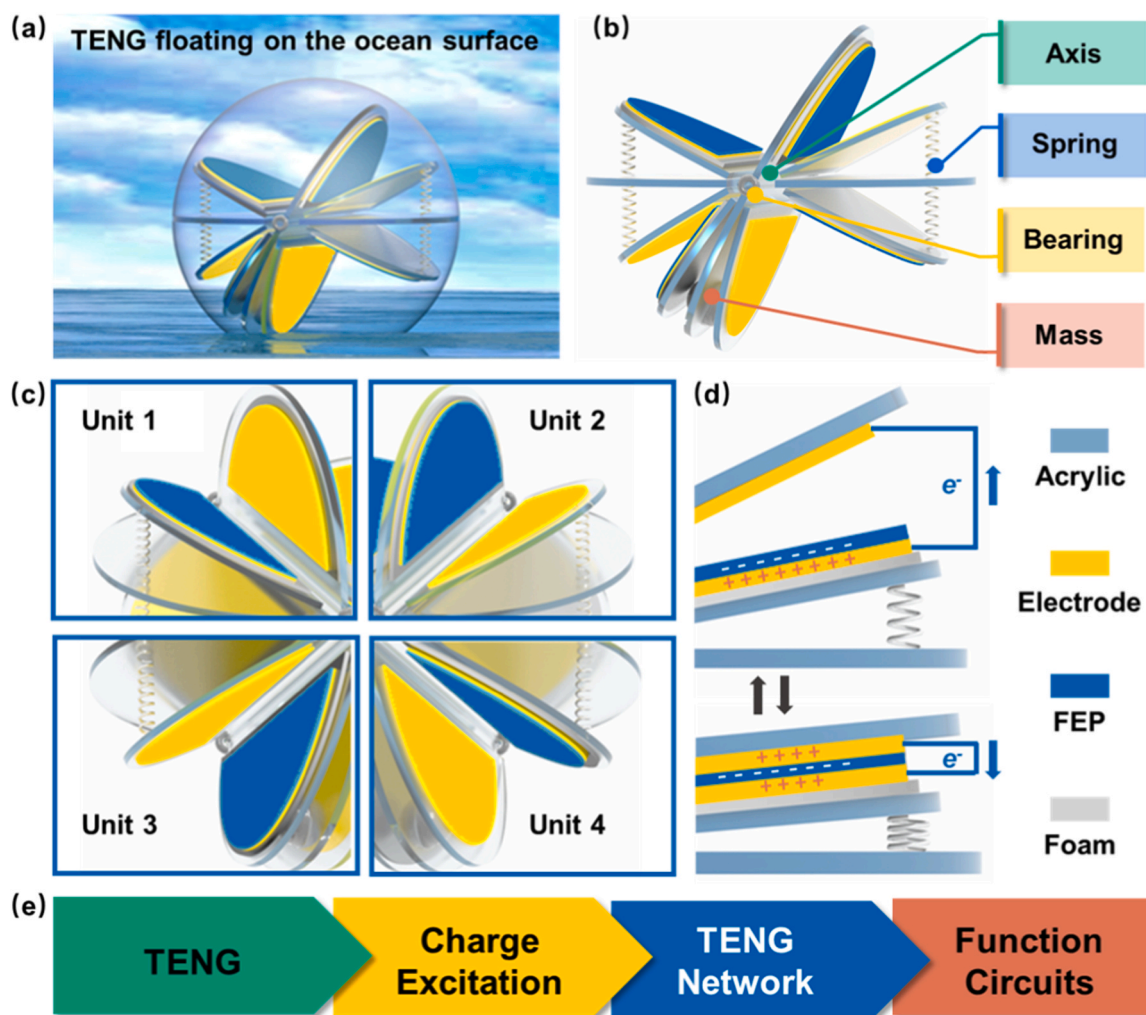
Fig. 1. (a) Schematic diagram of an as-fabricated spherical TENG with the spring-assisted swing structure floating on the ocean surface. (b) Schematic representation for the enlarged structure inside the TENG. (c) Relative positions of four basic units in the spherical TENG. (d) Schematic working principle of each basic unit. (e) Framework for constructing the self-powered system based on the charge excitation TENG network driven by the water waves.

applications toward blue energy. The charge excitation system reported in our recent work [29], based on the voltage-multiplying circuit (VMC), can be applied to improve the output current, thereby the output power.

In this work, we developed a new spherical TENG to harvest water wave energy, combining the advantages of the spring-assisted structure and swing structure. On the basis of structure optimization, the charge excitation circuit (CEC) was integrated with the TENG to boost the output current. First, the TENG was optimized by adjusting the spring length and the copper ball diameter in the structure. Next, the output performance of the optimal TENG was systematically studied under different water wave conditions generated by a standard wave tank equipment. Then, a TENG array consisting of four TENG units was fabricated and integrated with the CECs, and the output characteristics were measured correspondingly. Finally, the charge excitation TENG array was applied to power a digital thermometer and a wireless signal transmission and reception system, demonstrating potential applications of TENGs toward large-scale maritime internet of things (IoTs).

2. Experimental section

2.1. Fabrication of the TENG device

First, a circular acrylic sheet (diameter: 11 cm, thick: 2 mm) was fabricated by the laser cutting machine as the main part of the swing

component, and an axis (length: 12 cm) was integrated with it. A hole was cut out at the lower part of the circular acrylic sheet for placing the copper mass ball, and then two acrylic semicircular acrylic sheets were adopted to sandwich the copper ball. Through two commercial bearings, the swing component was adhered to the inner wall of the acrylic spherical shell (diameter: 12 cm). Second, the two spring components of the TENG device were fixed with the spherical shell through the semi-circular sheets in the middle. Springs on the top and bottom of the sheets were utilized to support acrylic pieces colliding with the swing component. Third, the Cu foils and FEP films (thick: 12.5 μm) bonded with other Cu electrodes were alternately pasted in the four spaces separated by these acrylic sheets, and foams were introduced under the Cu-FEP film. For each unit, electrons were pre-injected onto the surfaces of FEP films by the corona discharging method. Fourth, the units were divided into two sets, according to the motion phase. The units in one set were directly connected in parallel, while between the two sets, the series connection manner was adopted. At last, in order to avoid the adverse effect of the high humidity, the TENGs were waterproofed by the tile cement, which can keep the outputs with a slight decrease for a long time.

2.2. Electric measurements of the TENG device

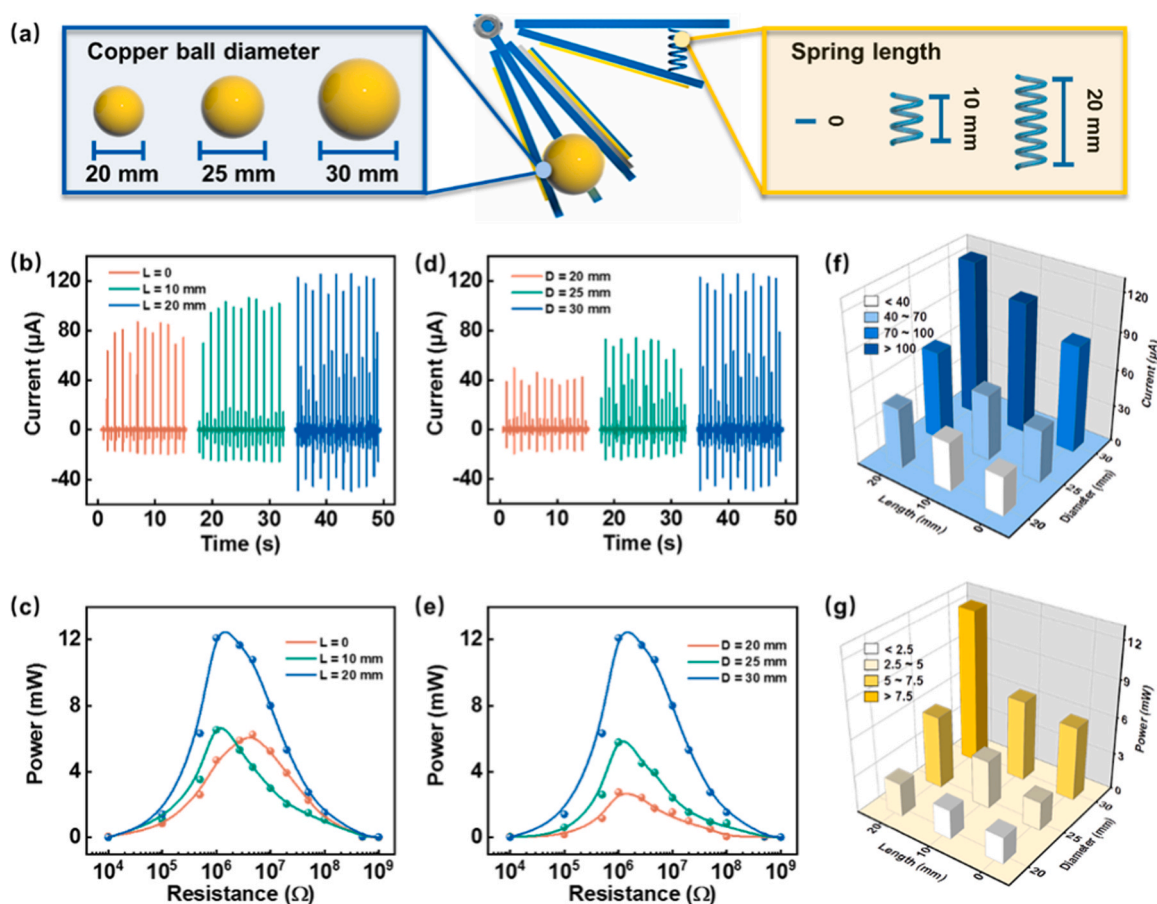The electrical outputs of the TENG device were measured under the

Fig. 2. (a) Sketches showing the copper balls with different diameters and springs with different lengths in the spherical TENG. (b) Output current and (c) output power-resistance profiles for various spring lengths at the copper ball diameter of 30 mm. (d) Output current and (e) output power-resistance profiles for various copper ball diameters at the spring length of 20 mm. (f-g) 3D graph summarizing the effects of spring length and copper ball diameter on (f) output current and (g) output power.

ideal triggering generated by a linear motor or the regular water waves generated by a standard wave tank equipment reported previously [30]. The equipment contains a wave generating mechanism and a rebound wave absorber. The output current, output voltage and transferred charge of the TENG devices, and charging voltage on capacitors were all measured by a current preamplifier (Keithley 6514 System Electrometer).

3. Results and discussion

3.1. Device structure and working principle

The spherical TENG coupling the spring-assisted structure and the swing structure, floating on the ocean surface, is schematically shown in Fig. 1a. The diameter of the outer acrylic spherical shell is 12 cm, and the inner part is separately demonstrated in Fig. 1b. The inner part contains a swing component and a spring component, whose details are indicated in the diagram. For the swing component, an axis is integrated with it, while two bearings are fixed at the inner wall of the spherical shell. A copper mass ball is embedded at the bottom of the component to lower the center of gravity for reinforcing the swing motion. For the spring component, two middle acrylic sheets are adhered to the spherical shell, which meanwhile support four movable acrylic sheets by springs. The photograph of an as-fabricated spherical TENG is presented in Fig. S1. Triggered by water waves, the spherical shell is subjected to external forces, inducing the swing component inside to swing left and right. The acrylic sheets supported by springs restrict the swing height and enhance the swing frequency.

This unique spherical TENG contains four TENG units, and the relative positions are labeled in Fig. 1c. Each unit is made of a copper foil as an electrode and a 12.5 μm-thick fluorinated ethylene propylene (FEP) film bonded with another copper foil as the dielectric layer. The flexible foam is introduced under the Cu-FEP film to improve the contact intimacy between the triboelectric materials. The detailed fabrication process can be found in the Experimental Section. The working mechanism of a TENG unit is briefly described in Fig. 1d. As the swing component swings, the contact and separation of the Cu electrode and FEP tribo-layer cause the accumulation of opposite charges on their respective surfaces. The change of electrical potential between the two electrodes during the movement causes charges flow through the external circuit. According to the relative positions of the four TENG units indicated in Fig. 1c, these units were divided into two sets shown in Fig. S2a. For one TENG set, the contact and separation in each unit are synchronized, so the units can be directly linked without rectifier bridges. The output voltage curves of the two TENG sets were respectively measured in Fig. S2b, illustrating that they hardly interfere with each other. Consequently, no matter whether the TENG sets are connected in parallel or series, the output offset will never occur. In this work, the series connection was adopted. For practical applications of the TENG, a self-powered energy harvesting system with high efficiency driven by water waves is needed to be constructed, whose framework is illustrated in Fig. 1e. Firstly, the TENG vibrates with the water waves, converting water kinetic energy to electrical outputs. Secondly, the output current of the TENG is boosted by the charge excitation circuit (CEC). Then, multiple charge excitation TENGs are linked together to compose a TENG network for large-scale water wave energy harvesting.
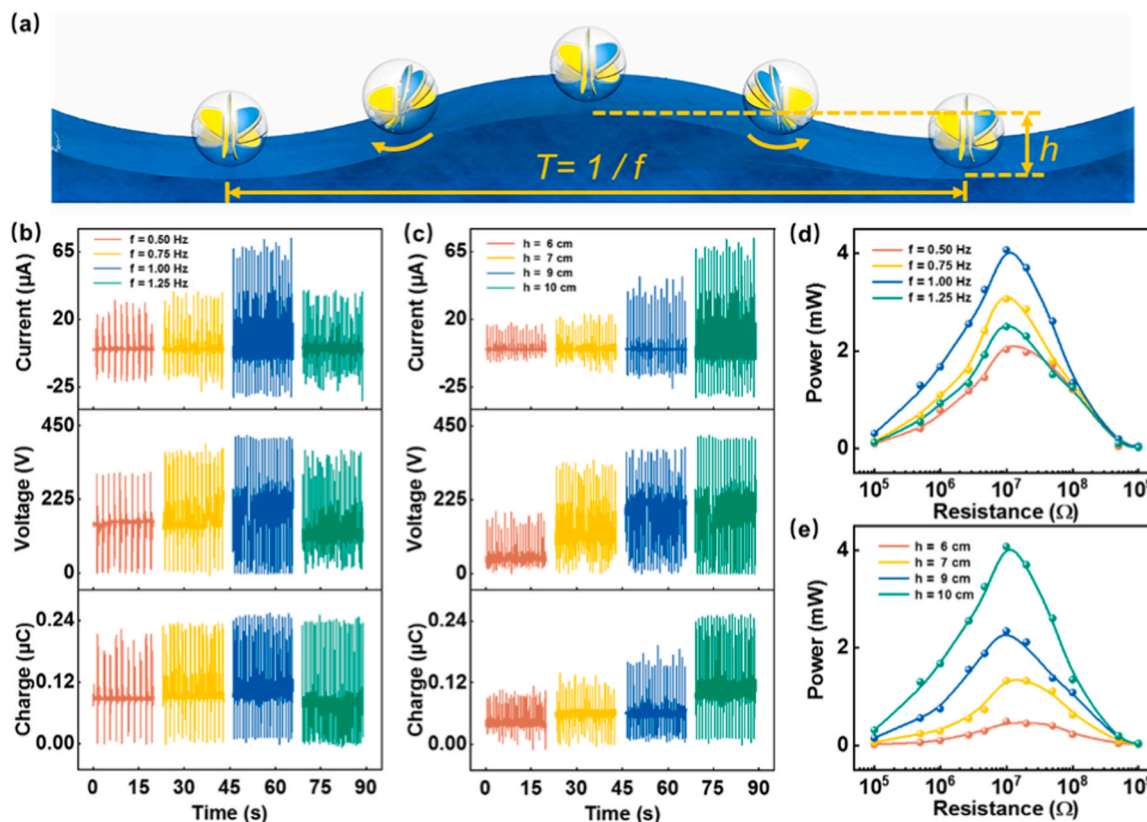
Fig. 3. (a) Schematic scene exhibiting various motion patterns of the spherical TENG in the water waves generated by the standard wave tank equipment. (b) Output current, output voltage and transferred charge at different water wave frequencies. The wave height is maintained as 10 cm. (c) Output current, output voltage and transferred charge at different water wave heights. The wave frequency is maintained as 1 Hz. (d-e) Influences of (d) wave frequency and (e) wave height on the output power-resistance relationships.

Finally, the charge excitation TENG network can be applied to power a series of function circuits, including sensing, displaying and signal transmitting, etc.

3.2. TENG structure optimization

The spring length and copper ball diameter in the TENG device structure are the two most crucial parameters governing the output performance of the TENG, which are clearly depicted in Fig. 2a. To systematically explore the influences of these two factors, a linear motor was utilized to drive the TENG regularly, fixing the vibrating frequency at 1 Hz and the amplitude at 10 cm. As the spring length L increases from zero to 20 mm (the copper ball diameter D = 30 mm), the output current, peak power and transferred charges were investigated in Figs. 2b, 2c and S3a. At the longest spring length (L = 20 mm), the TENG achieves the maximum output current of 125.3 µA, peak power of 12.1 mW and transferred charge of 0.2 µC. Besides the magnitude of the output peaks, the frequency is also enhanced by the springs, which can be reflected by the obvious increase of the peak density in Fig. 2b. Before reaching the highest point of the free movement, the swing component collides with the spring component elastically, causing the swing period to decrease and the frequency to increase. The results prove that the existence of the springs can not only improve the contact force between the triboelectric materials in each TENG unit, but also strengthen the reciprocation of the swing component. However, the longer springs were not discussed due to the limitation of spherical shell space.

Another important factor is the size or weight of the copper ball in the TENG structure, affecting the barycenter of the swing component. The trends of the output current, output power and transferred charge with the copper ball diameter D raising from 20 mm to 30 mm were

studied in Figs. 2d, 2e and S3b (the spring length L = 20 mm). The maximum output performance is achieved when D = 30 mm, since the heavy copper ball aggravates the deviation of the barycenter and increases the inertia of the swing movements. Nevertheless, larger balls are not advisable to ensure the enough space for swing motions. In order to present the combined effect of these two factors of spring length and copper ball diameter, an orthogonal experiment was prepared and the results are summarized in Figs. 2f and 2g. The spring length of 20 mm and copper ball diameter of 30 mm are confirmed as the optimal structure parameters, and the maximum output current and output power reach 125.3 µA and 12.1 mW, respectively. The output voltage of the optimal TENG was measured as shown in Fig. S4.

3.3. Performance of the TENG in water

For investigating the output performance of the TENG in real water waves, the TENG was placed and tested in a standard wave tank equipment [30]. Driven by water waves, the swing component in the TENG structure swings and collides with the spring component, whose patterns are schematically depicted in Fig. 3a. In this work, the influences of the water wave frequency and height were systematically studied, and the frequency and height are specifically expressed in Fig. 3a. The trends of the output current, output voltage and transferred charge at various water wave frequencies from 0.5 Hz to 1.25 Hz are shown in Fig. 3b, when fixing the wave height as 10 cm. As the frequency increases, the output performances first increase then decrease, reaching the maximum output current of 56.7 µA, output voltage of 419 V and transferred charge of 0.25 µC at the frequency of 1 Hz. Furthermore, the trend of the output power in Fig. 3d is the same, and the peak value of 4.1 mW at the matched resistance of 10 MΩ is also
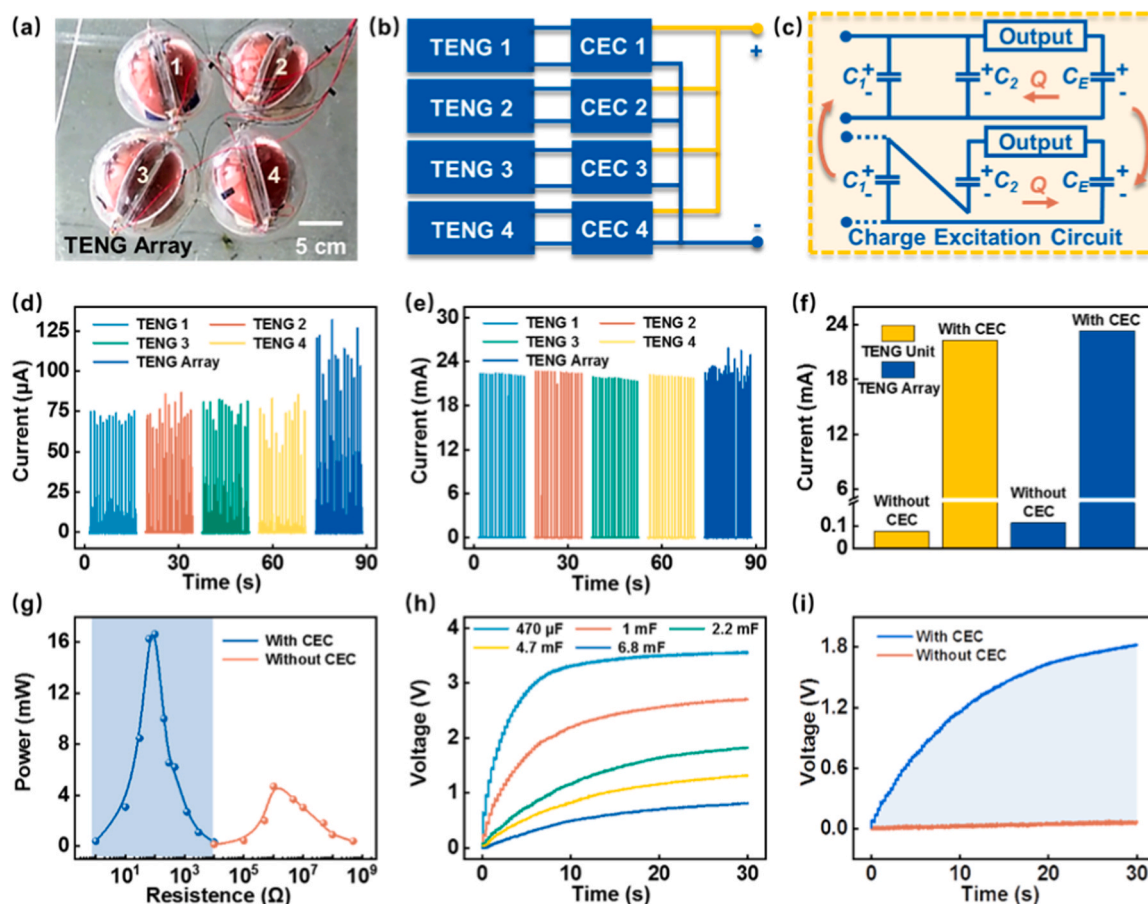
Fig. 4. (a) Photograph of an as-fabricated TENG array floating on the water surface, which is composed of four TENGs linked by rigid strings. (b) Circuit diagram of the TENG array connected by the CECs. (c) Schematic working principle of the CEC. (d-e) Individual output current of each TENG in the array and the overall output current of the whole array (d) without or (e) with CECs. (f) Comparison for the output current of the TENG array with or without the CECs. (g) Power-resistance relationships of the TENG array with or without the CECs. (h) Voltage curves on the capacitors for the TENG array integrated with the CECs when charging different capacitors. (i) Comparison for the charging profiles of the TENG array with or without the CECs.

achieved at the frequency of 1 Hz. The initial increase is due to the faster impact of the two components in the TENG structure. When the frequency is higher than 1 Hz, the swing period is not long enough for the swing component to press the spring component sufficiently, leading to the following drop of the electrical outputs.

In addition, the effects of the wave height on the output characteristics of the TENG were also studied. As can be seen in Fig. 3c, at the optimal frequency of 1 Hz, the output current, output voltage and transferred charge all increase with increasing the wave height, implying that higher water waves are beneficial to the TENG operation. The power-resistance relationships at various wave heights are displayed in Fig. 3e, and the maximum power value of 4.1 mW at the matched resistance of 10 MΩ is realized at the highest wave height. The output performance is inferior at the low wave height, because the slight waves cannot fully drive the TENG device due to its own weight.

3.4. Charge excitation TENG array

In order to capture water wave energy in a larger scale, a TENG array consisting of four single TENGs was fabricated and investigated under the optimal water wave conditions just discussed. The photograph of the TENG array floating on the water surface is exhibited in Fig. 4a. The four TENGs were structurally linked by rigid strings and electrically connected in parallel through rectifier bridges, and the circuit diagram is shown in Fig. S5. In Fig. 4d, the rectified output current of each TENG in the array was separately measured, and the levels are almost the same and around 75.0 μA, which is slightly higher than that of single TENG as

shown in Fig. 3b. As for the whole TENG array, the overall output current of the four TENGs connected in parallel is also presented in Fig. 4d. Not only the output current value is improved to 113.0 μA, but also the peak density is simultaneously increased, ascribed to the incomplete superposition of the TENG outputs.

To further improve the output performance of the TENG array, the charge excitation circuit (CEC) reported in our recent work was applied to integrate with the TENG array [29]. The working mechanism of the CEC is simply described in Fig. 4c. The TENG can control the connection mode of the capacitor group (C_1, $C_2 = 10$ μF) to switch between parallel and series through metal-oxide-semiconductor field effect transistors (MOSFETs), resulting in the varying voltage difference with the external capacitor C_E (1 mF), whose capacitance is much larger than that of the capacitor group to maintain a stable voltage value. The voltage difference drives charges to flow back and forth between the capacitor group and the C_E, and the current of this process is greatly higher than that produced by ordinary TENGs. For reaching the working voltages of the components in the CECs, the CECs have to be pre-charged by the TENGs for about 35 min. The pre-charging time can be hardly shortened, unless the transferred charges of the TENGs themselves are improved, but we can pre-charge the CEC by a DC source before using it. The photograph of the electrical components integrated on a circuit board (4 cm × 4 cm) is displayed in Fig. S6. The output current of a single charge excitation TENG was tested in Fig. S7, indicating a peak current of about 7.0 mA.

The connection manner of the TENG array and the CECs is illustrated in Fig. 4b. Each TENG in the array is first integrated with a CEC separately, and then connected with each other in parallel. A CEC can only be
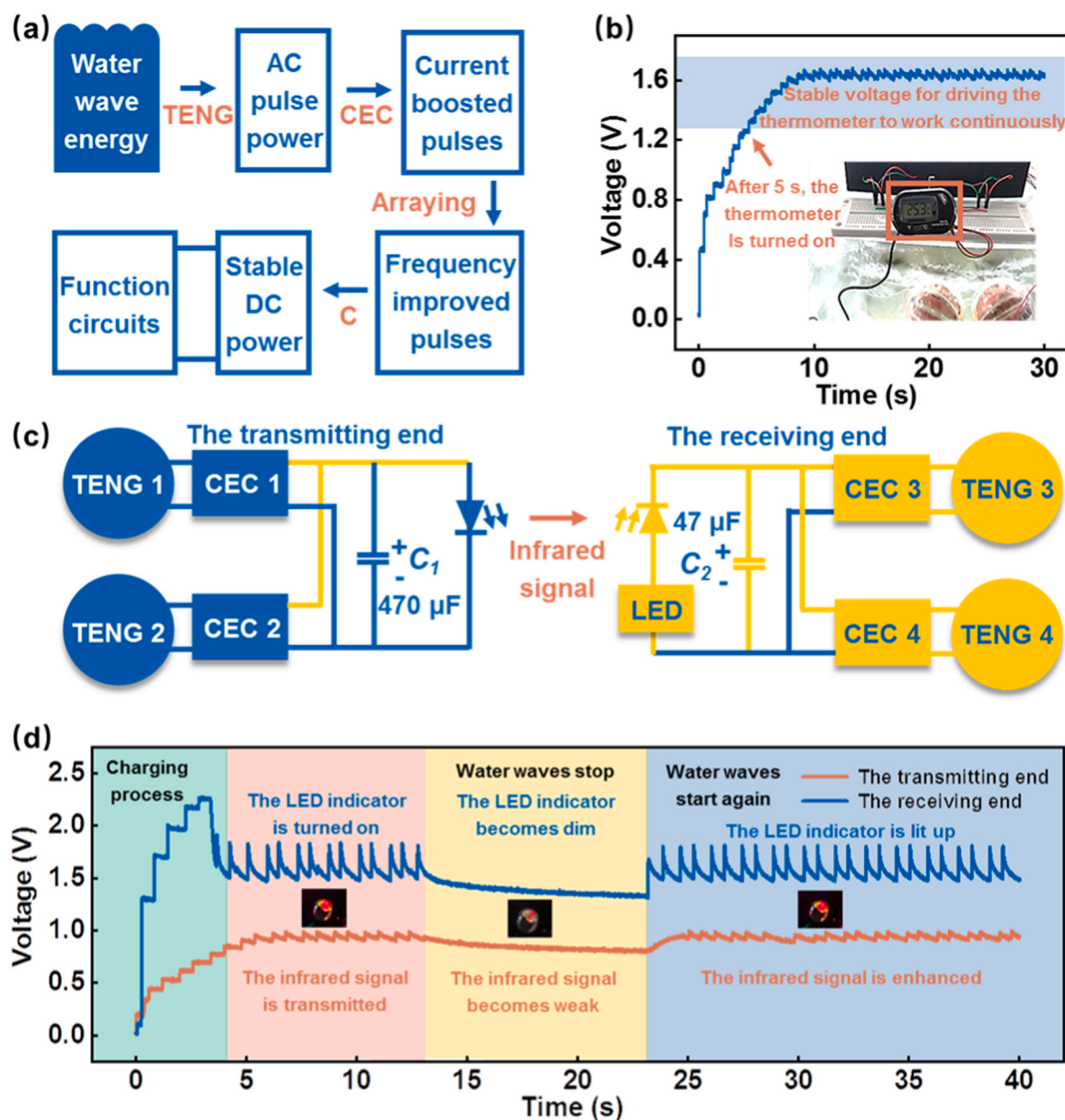
Fig. 5. (a) Flow chart of utilizing the charge excitation TENG array to drive a series of function circuits. (b) Application demonstration for powering a digital thermometer. The voltage profiles on the thermometer and the photograph of the CECs and LCD screen are shown. (c) Simplified circuit diagram of the self-powered wireless signal transmission and reception system. (d) Voltage profiles on the transmitting end and receiving end, and photographs of the LED indicator at different stages.

integrated with a single unit of the TENG array rather than the whole array. If the TENG units are first connected together through rectifier bridges and then equipped with a CEC, the DC output cannot make the CEC properly work and even damages the components in it. Fig. 4e exhibits the individual output current for each TENG with a CEC, and the peak value is up to 22.3 mA. The overall output current for the whole TENG array is only improved a little to 23.3 mA, but the current peak density is significantly increased, as shown in the rightest part of Fig. 4e. In order to reveal the influences of the CECs on the TENG array, the output currents with or without CECs are summarized in Fig. 4f for comparison. With the CECs, the average output currents for single TENGs in the array and the overall output current for the entire TENG array can be respectively increased by 295 times and 205 times. Moreover, the CECs can also increase the output power of the TENG array. The power-resistance relationships of the TENG array with or without the CECs are displayed in Fig. 4g. The integrating of the CECs improves the peak power by 2.5 times from 4.69 mW to 16.64 mW, while the

matched resistance is decreased from 1 MΩ to 100 Ω. Here, the average power corresponding to the maximum peak power is calculated as 1.2 mW. The small capacitances of TENGs always cause high internal impedances and matched resistances. The integration of the CECs significantly increases the capacitances of the TENG array, so the internal impedance and matched resistance decrease accordingly. The charging performances of the TENG array with the CECs to various capacitors from 470 μF to 6.8 mF in 30 s are presented in Fig. 4h. For all capacitances, the voltage curves rapidly increase in the initial period, and then gradually stabilize, implying the pulse output is transferred into the stable direct current (DC) output. The voltage values after charging for 30 s are associated with the capacitances, and larger values can be achieved for smaller capacitances. Fig. 4i is the comparison graph of charging a 2.2 mF capacitor directly or integrated with the CECs, exhibiting 10 times improvement of charging speed.

3.5. Application demonstration

Finally, the applications of charge excitation TENG array for water wave energy harvesting were demonstrated. The flow chart of utilizing the TENG array with the CECs to drive a series of function circuits is explained in Fig. 5a. The TENG first converts the mechanical energy of the water wave motions to alternating current (AC) pulse electrical power. Integrated with the CEC, the output current is boosted, and the AC pulses are transferred to DC pulses simultaneously. Through organizing multiple TENGs into an array or network, the density of output signals can be greatly increased. In order to satisfy the demands of general applications, a suitable capacitor is required for stable DC power. Fig. 5b is the voltage curve of the charge excitation TENG array when powering a digital thermometer under the optimal water wave conditions. Here, a capacitor of 47 μF is applied, and it only takes 5 s to reach the working voltage of 1.2 V for the thermometer. The photograph of lit-up liquid crystal display (LCD) screen of the thermometer is presented in the inset of Fig. 5b. After reaching the working voltage, the voltage curve stabilizes at 1.6 V, so the thermometer can work constantly with the water waves. After the water waves stop, the thermometer will keep working for a short time until the stored energy in the capacitor is exhausted. The experimental process was recorded in Video S1.

Supplementary material related to this article can be found online at doi:10.1016/j.nanoen.2021.105836.

Besides the thermometer, a self-powered wireless signal transmission and reception system based on the charge excitation TENG array was designed for the application demonstration. The circuit diagram of this system is depicted in Fig. 5c, containing a transmitting end and a receiving end. At the transmitting end, two charge excitation TENGs in the array power an infrared emitting diode through charging a 470 μF capacitor. At the receiving end, the other two TENGs power the relevant infrared receiving diode and a liquid emitting diode (LED) indicator through charging a 47 μF capacitor. The voltage curves of the two ends are both displayed in Fig. 5d. In the first 4 s, the voltage on the transmitting end gradually rises to the working voltage of the infrared emitting diode. For the receiving end, the TENGs with the CECs only charges the capacitor in this process, since the infrared receiving diode is cut off. Then, the transmitting end maintains the voltage of 1.0 V, and emits infrared signal continuously. Correspondingly, the receiving end accepts the signal, making the voltage rapidly decrease to the working voltage of the LED, and the lit-up LED indicator is shown in the inset. At 14 s, the water wave tank equipment is stopped, so the stored energy in the capacitors at the two ends is slowly dissipated. The intensity of the infrared signal becomes weak and the LED indicator becomes dim. When the water waves start again, the system is recovered to the normal working condition, enhancing the infrared signal and lighting up the LED. The experimental process was recorded in Video S2.

Supplementary material related to this article can be found online at doi:10.1016/j.nanoen.2021.105836.

4. Conclusion

In summary, we designed and fabricated a new spherical TENG based on the spring-assisted swing structure for the water wave energy harvesting, and integrated it with the charge excitation circuit. Under the regular triggering generated by the linear motor, the output performance was optimized by adjusting the structural parameters, such as the spring length and the copper ball diameter inside the TENG. When triggered by real water waves, the outputs of the TENG were found to be determined by the water wave frequency and height. The maximum output current of 56.2 μA and output power of 4.1 mW were achieved under the water wave conditions of 1.0 Hz and 10 cm. Furthermore, four TENGs integrated with CECs were connected into a charge excitation TENG array, having an improved output current of up to 23.3 mA and an output power of 16.6 mW. Finally, the charge excitation TENG array

was utilized to power a digital thermometer and a wireless signal transmission and reception system without external power supply for self-powered systems, demonstrating the application prospects in remote environmental information monitoring and transmitting toward blue energy.

CRediT authorship contribution statement

Xi Liang: Conceptualization, Methodology, Visualization, Data curation, Writing-original draft. **Zhirong Liu:** Methodology, Validation, Writing-review & editing. **Yawei Feng:** Methodology, Resources, Writing-review & editing. **Jiajia Han**: Methodology, Visualization. **Linlin Li:** Resources, Methodology. **Jie An:** Resources, Methodology. **Pengfei Chen:** Resources, Methodology. **Tao Jiang:** Conceptualization, Methodology, Supervision, Writing-review & editing. **Zhong Lin Wang:** Conceptualization, Supervision, Writing-review & editing.

Declaration of Competing Interest

The authors declare that they have no known competing financial interests or personal relationships that could have appeared to influence the work reported in this paper.

Acknowledgments

Appendix A. Supporting information

Supplementary data associated with this article can be found in the online version at doi:10.1016/j.nanoen.2021.105836.

References

[1] J.P. Painuly, Barriers to renewable energy penetration; a framework for analysis, Renew. Energy 24 (2001) 73–89.
[2] Z.L. Wang, Catch wave power in floating nets, Nature 524 (2017) 159–160.
[3] S.P. Beeby, R.N. Torah, M.J. Tudor, P. Glynne-Jones, T. O'Donnell, C.R. Saha, S. Roy, A micro electromagnetic generator for vibration energy harvesting, J. Micromech. Microeng. 17 (2007) 1257–1265.
[4] Z. Wu, H. Guo, W. Ding, Y. Wang, L. Zhang, Z.L. Wang, A hybridized triboelectric-electromagnetic water wave energy harvester based on a magnetic sphere, ACS Nano 13 (2019) 2349–2356.
[5] X. Wang, Y. Yang, Effective energy storage from a hybridized electromagnetic-triboelectric nanogenerator, Nano Energy 32 (2017) 36–41.
[6] F.-R. Fan, Z.-Q. Tian, Z.L. Wang, Flexible triboelectric generator!, Nano Energy 1 (2012) 328–334.
[7] W. Wang, Y. Wu, Z. Chang, F. Chen, H. Wang, G. Gu, H. Zheng, G. Cheng, Z. L. Wang, Self-powered intelligent water meter for electrostatic scale preventing, rust protection, and flow sensor in a solar heater system, ACS Appl. Mater. Interfaces 11 (2019) 6396–6403.
[8] Z.L. Wang, On Maxwell's displacement current for energy and sensors: the origin of nanogenerators, Mater. Today 20 (2017) 74–82.
[9] X. Wang, S. Niu, F. Yin, F. Yi, Z. You, Z.L. Wang, Triboelectric nanogenerator based on fully enclosed rolling spherical structure for harvesting low-frequency water wave energy, Adv. Energy Mater. 5 (2015) 1501467.
[10] L. Zhang, C. Han, T. Jiang, T. Zhou, X. Li, C. Zhang, Z.L. Wang, Multilayer wavy-structured robust triboelectric nanogenerator for harvesting water wave energy, Nano Energy 22 (2016) 87–94.
[11] T. Xiao, T. Jiang, J. Zhu, X. Liang, L. Xu, J. Shao, C. Zhang, J. Wang, Z.L. Wang, Silicone-based triboelectric nanogenerator for water wave energy harvesting, ACS Appl. Mater. Interfaces 10 (2018) 3616–3623.
[12] H. Wang, Q. Zhu, Z. Ding, Z. Li, H. Zheng, J. Fu, C. Diao, X. Zhang, J. Tian, Y. Zi, A fully-packaged ship-shaped hybrid nanogenerator for blue energy harvesting toward seawater self-desalination and self-powered positioning, Nano Energy 57 (2019) 616–624.
[13] X. Yang, L. Xu, P. Lin, W. Zhong, Y. Bai, J. Luo, J. Chen, Z.L. Wang, Macroscopic self-assembly network of encapsulated high-performance triboelectric

nanogenerators for water wave energy harvesting, Nano Energy 60 (2019) 404–412.

[14] P. Cheng, H. Guo, C. Zhang, X. Yin, X. Li, D. Liu, W. Song, X. Sun, J. Wang, Z. L. Wang, Largely enhanced triboelectric nanogenerator for efficient harvesting of water wave energy by soft contacted structure, Nano Energy 57 (2019) 432–439.

[15] Y. Bai, L. Xu, C. He, L. Zhu, X. Yang, T. Jiang, J. Nie, W. Zhong, Z.L. Wang, High-performance triboelectric nanogenerators for self-powered, in-situ and real-time water quality mapping, Nano Energy 66 (2019), 104117.

[16] Z. Ren, Z. Wang, Z. Liu, L. Wang, H. Guo, L. Lin, S. Li, X. Chen, W. Tang, Z.L. Wang, Energy harvesting from breeze wind (0.7–6 m s^{-1}) using ultra-stretchable triboelectric nanogenerator, Adv. Energy Mater. 10 (2020), 2001770.

[17] W. Liu, L. Xu, T. Bu, H. Yang, G. Liu, W. Li, Y. Pang, C. Hu, C. Zhang, T. Cheng, Torus structured triboelectric nanogenerator array for water wave energy harvesting, Nano Energy 58 (2019) 499–507.

[18] X. Liang, T. Jiang, G. Liu, T. Xiao, L. Xu, W. Li, F. Xi, C. Zhang, Z.L. Wang, Triboelectric nanogenerator networks integrated with power management module for water wave energy harvesting, Adv. Funct. Mater. 29 (2019), 1807241.

[19] Y. Xi, H. Guo, Y. Zi, X. Li, J. Wang, J. Deng, S. Li, C. Hu, X. Cao, Z.L. Wang, Multifunctional TENG for blue energy scavenging and self-powered wind-speed sensor, Adv. Energy Mater. 7 (2017), 1602397.

[20] N. Wang, J. Zou, Y. Yang, X.Y. Li, Y. Guo, C. Jiang, X. Jia, X. Cao, Kelp-inspired biomimetic triboelectric nanogenerator boosts wave energy harvesting, Nano Energy 55 (2019) 541–547.

[21] C. Rodrigues, D. Nunes, D. Clemente, N. Mathias, J.M. Correia, P. Rosa-Santos, F. Taveira-Pinto, T. Morais, A. Pereira, J. Ventura, Emerging triboelectric nanogenerators for ocean wave energy harvsting: state of the art and future perpectives, Energy Environ. Sci. 13 (2020) 2657–2683.

[22] D.Y. Kim, H.S. Kim, D.S. Kong, M.K. Choi, H.B. Kim, J.H. Lee, G. Murillo, M. Lee, S. S. Kim, J.M. Jung, Emerging triboelectric nanogenerators for ocean wave energy harvsting: state of the art and future perpectives, Nano Energy 45 (2018) 247–254.

[23] H. Yang, M. Deng, Q. Zeng, X. Zhang, J. Hu, Q. Tang, H. Yang, C. Hu, Y. Xi, Z. L. Wang, Polydirectional microvibration energy collection for self-powered multifunctional systems based on hybridized nanogenerators, ACS Nano 14 (2020) 3328–3336.

[24] T. Jiang, H. Pang, J. An, P. Lu, Y. Feng, X. Liang, W. Zhong, Z.L. Wang, Robust swing-structured triboelectric nanogenerator for efficient blue energy harvesting, Adv. Energy Mater. 10 (2020), 2000064.

[25] Z. Lin, B. Zhang, H. Guo, Z. Wu, H. Zou, J. Yang, Z.L. Wang, Super-robust and frequency-multiplied triboelectric nanogenerator for efficient harvesting water and wind energy, Nano Energy 64 (2019), 103908.

[26] T. Jiang, Y. Yao, L. Xu, L. Zhang, T. Xiao, Z.L. Wang, Spring-assisted triboelectric nanogenerator for efficiently harvesting water wave energy, Nano Energy 31 (2017) 560–567.

[27] T. Xiao, X. Liang, T. Jiang, L. Xu, J. Shao, J. Nie, Y. Bai, W. Zhong, Z.L. Wang, Spherical triboelectric nanogenerators based on spring-assisted multilayered structure for efficient water wave energy harvesting, Adv. Funct. Mater. 28 (2018), 1802634.

[28] Y. Feng, T. Jiang, X. Liang, J. An, Z.L. Wang, Cylindrical triboelectric nanogenerator based on swing structure for efficient harvesting of ultra-low-frequency water wave energy, Appl. Phys. Rev. 7 (2020), 021401.

[29] X. Liang, T. Jiang, Y. Feng, P.J. Lu, J. An, Z.L. Wang, Triboelectric nanogenerator network integrated with charge excitation circuit for effective water wave energy harvesting, Adv. Energy Mater. 10 (2020), 2002123.

[30] J. An, Z. Wang, T. Jiang, X. Liang, Z.L. Wang, Whirling-folded triboelectric nanogenerator with high average power for water wave energy harvesting, Adv. Funct. Mater. 29 (2019), 1904867.

Xi Liang received her B.S. degree in Material Science and Engineering from China University of Geoscience in 2016. Now she is a Ph.D. candidate in Beijing Institute of Nanoenergy and Nanosystems, Chinese Academy of Sciences. Her research interests are focused on blue energy harvesting and self-powered systems.

Zhirong Liu received her B.S. degree from China University of Geosciences in 2016. Currently she is a Ph.D candidate supervised by Prof. LinLin Li in Beijing Institute of Nanoenergy and Nanosystem, Chinese Academy of Science. Her research interests are mainly focused on bioactive nanomaterials/nano-devices for biomedical applications in drug delivery, stem cell manipulation and tissue regeneration.

Yawei Feng received his master degree in Industrial Catalysis from Shanghai Normal University in 2018, and he is currently pursuing his Ph.D. degree in Beijing Institute of Nanoenergy and Nanosystems, Chinese Academy of Sciences. His research interests are focused on the nanogenerator, self-powered chemistry and the coupling of piezotronics/piezo-phototronics and catalysis.

Jiajia Han received her B.S. degree in Chemistry from Henan Normal University in 2019, and she is currently pursuing a M.S. degree in Beijing Institute of Nanoenergy and Nanosystems, Chinese Academy of Sciences. Her research interests are focused on blue energy harvesting and self-powered systems.
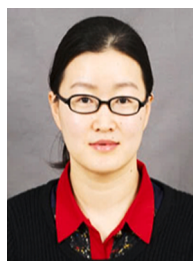
Prof. Linlin Li received her M.S. degree in Biochemistry and Molecular Biology from Beijing Normal University in 2005, and Ph.D. degree in Physical Chemistry from Technical Institute of Physics and Chemistry, Chinese Academy of Sciences, in 2008. Currently, she is a professor in Beijing Institute of Nanoenergy and Nanosystems, CAS. Her research interests include biomedical applications of biomaterials and devices (nanogenerators and piezotronic devices) in cancer therapy, biosensing, and tissue regeneration.
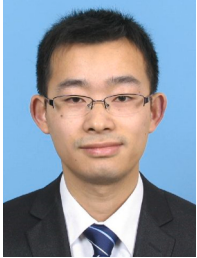

Jie An received his B.S. degree in Maritime Engineering from Dalian Maritime University in 2017. Now he is pursuing his Ph. D. degree in Beijing Institute of Nanoenergy and Nanosystems, Chinese Academy of Sciences. His research interests are mainly focused on clean energy harvesting and self-powered sensor systems based on triboelectric nanogenerator.

Pengfei Chen received his B.S. degree at Dalian Maritime University in 2018. Now he is a Ph.D. candidate in Beijing Institute of Nanoenergy and Nanosystem, Chinese Academy of Science. His research interests are focused on blue energy harvesting and self-powered sensing.

Dr. Tao Jiang is a professor in the Beijing Institute of Nanoenergy and Nanosystems, Chinese Academy of Sciences. He received his B.S. and Ph.D. degrees from School of Materials Science and Engineering, in 2008 and 2014, respectively, from East China University of Science and Technology. After graduation, he worked in the Beijing Institute of Nanoenergy and Nanosystems as a postdoctoral research fellow. His research interests are the theoretical studies of triboelectric nanogenerators, and practical applications in blue energy harvesting.

Prof. Zhong Lin Wang received his Ph.D. degree from Arizona State University in physics. He now is the Hightower Chair in Materials Science and Engineering, Regents' Professor at Georgia Tech, the chief scientist and director of the Beijing Institute of Nanoenergy and Nanosystems, Chinese Academy of Sciences. Prof. Wang has made original and innovative contributions to the synthesis, discovery, characterization and understanding of fundamental physical properties of oxide nanobelts and nanowires, as well as applications of nanowires in energy sciences, electronics, optoelectronics and biological science. His discovery and breakthroughs in developing nanogenerators establish the principle and technological road map for harvesting mechanical energy from environmental and biological systems for powering personal electronics. His research on self-powered nanosystems has inspired the worldwide efforts in academia and industry for studying energy for micro-nano-systems, which is now a distinct disciplinary in energy research and future sensor networks. He coined and pioneered the fields of piezotronics and piezophototronics by introducing piezoelectric potential gated charge transport process in fabricating new electronic and optoelectronic devices.